Structural Engineering and Mechanics, *Vol. 75, No. 3 (2020) 377-387*
DOI: https://doi.org/10.12989/sem.2020.75.3.377

A simplified method for determining the acceleration amplitudes of long-span floor system under walking/running loads

Liang Cao*[1,2] and Y. Frank Chen[1, 3a]

[1]*School of Civil Engineering, Chongqing University, Chongqing, China*
[2]*Key Laboratory of New Technology for Construction of Cities in Mountain Area (Chongqing University), Ministry of Education, Chongqing 400045, China*
[3]*Department of Civil Engineering, The Pennsylvania State University, Middletown, PA, USA*

(Received January 25, 2020, Revised February 19, 2020, Accepted March 9, 2020)

Abstract. Modern long-span floor system typically possesses low damping and low natural frequency, presenting a potential vibration sensitivity problem induced by human activities. Field test and numerical analysis methods are available to study this kind of problems, but would be inconvenient for design engineers. This paper proposes a simplified method to determine the acceleration amplitudes of long-span floor system subjected to walking or running load, which can be carried out manually. To theoretically analyze the acceleration response, the floor system is simplified as an anisotropic rectangular plate and the mode decomposition method is used. To facilitate the calculation of acceleration amplitude a_P, a coefficient α_{wmn} or α_{Rmn} is introduced, with the former depending on the geometry and support condition of floor system and the latter on the contact duration t_R and natural frequency. The proposed simplified method is easy for practical use and gives safe structural designs.

Keywords: human activities, vibration serviceability, long-span floor, mode decomposition method, simplified analytical method

1. Introduction

In recent years, the long-span floor system with high-strength and light-weight material has been increasingly used in buildings, sport facilities and airport terminals, as it is the structurally desirable (Chen *et al*. 2016; Rana *et al*. 2015). For such floor system, the damping and natural frequency are generally low, resulting in a potential vibration perceptibility problem induced by human activities (Chen *et al*. 2013, Liu *et al*. 2019, 2020, Lu et al. 2012, Zivanovic *et al*. 2005, Zhou *et al*. 2016a), such as walking (Cao *et al*. 2018b, Shahabpoor *et al*. 2017), running (An *et al*. 2016) and jumping (Brownjohn *et al*. 2016). Among the various human activities, walking and running are regard as most common. If the dominant frequency of walking or running is close to the fundamental natural frequency of floor system, an excessive vibration will occur and may cause annoyance and discomfort to occupants. Taking Nya Ullevi Stadium as an example, the enthusiastic audience jumped in accordance with the songs, but unfortunately caused severe vibrations on the ground and structure in 1985 (Bodare and Erlingsson 1993). To avoid such undesirable situations, a further study on the subject is warranted.

Evaluating the vibration serviceability of a floor due to human activities is essential to the structural design. Several relevant vibration acceptability criteria have been proposed including the AISC Design Guide #11 (Murray *et al*. 1997, 2016), GB 50010-2010 (2010), JGJ 3-2010 (2010) and PCI Handbook (Wilden *et al*. 2010), which have assisted structural designers to complete their designs. In reviewing these criteria, acceleration threshold appears to be the main parameter. An easy and convenient calculation method for acceleration amplitude would be practically significant. For example, the acceleration amplitude a_p due to walking, jumping and rhythm excitations may be estimated by Eqs. (1), (2) and (3), respectively (Murray *et al*. 1997, 2016, Liu *et al*. 2018)

$$a_p = \frac{gP_0 e^{-0.35 f_n}}{\beta W} \quad \text{for walking excitation} \tag{1}$$

$$a_p = \frac{4\beta_J e^{-0.35 f_n} gG}{qab\pi} \quad \text{for individual jumping excitation} \tag{2}$$

$$a_p = g\frac{1.3}{2\beta_m} \cdot \frac{\alpha_i w_p}{w_t} \quad \text{for rhythm excitation} \tag{3}$$

where g is the gravity acceleration, P_0 is a constant force set as 0.29 kN and 0.41 kN respectively for floors and footbridges, f_n is the floor's natural frequency, β and β_m are the damping ratios, W is the floor's effective weight, β_J is a constant coefficient set as 4341.04 and 17548.53 respectively for girder and slab, α_i is the dynamic coefficient (Table 1) and w_p and w_t are respectively the effective weights per unit area of the participants distributed over floor and the floor.

In Eqs. (1)-(3), a_p is essentially a function of the natural

*Corresponding author, Professor
E-mail: liangcao@cqu.edu.cn
[a] Professor

ISSN: 1225-4568 (Print), 1598-6217 (Online)

Table 1 Values of dynamic coefficient α_i

Human activity	ith harmonic	α_i
Dancing	1st	0.5
Lively concert or sports event	1st	0.25
	2nd	0.05
Jumping exercise	1st	1.5
	2nd	0.6
	3rd	0.1

frequency (or stiffness) of floor system without considering different boundary conditions and vibration resonance. They are not suitable to calculate the vibration response induced by running excitation. So, this study proposes a simplified formula to calculate the peak acceleration induced by walking or running, which considers the boundary condition and natural frequency (resonant or not) of the floor system. The organization of this paper is as follows: first, the acceleration response of the floor system is obtained by the mode decomposition method; second, the coefficient α_{wmn} depending on the geometry and support condition of floor system and the coefficient α_{Rmn} depending on the contact duration and natural frequency of floor system are obtained to derive the simplified formula; finally, specific coefficients $C_w\alpha_{wi}/C_s$, $a_{wi}\omega_i^2/\left|\omega_i^2-\omega_{mn}^2\right|$ (i=1, 2, 3, 4), $1/\left|\pi^2-(t_R\omega_{mn})^2\right|$ are presented to calculate the peak acceleration a_p induced by walking or running excitation.

2. Walking and running forcing function

For theoretically analyzing the acceleration response of the floor system subjected to walking excitation, several walking forcing functions have been considered, such as the stochastic model (Racic and Brownjohn 2011), biodynamic walking model (Da Silva and Pimentel 2011), agent-based model (Shahabpoor *et al*. 2018) and Fourier load function (Wang and Chen 2017). For practical convenience, the Fourier load function (Fig. 1) is used in this study, which is described by (Smith *et al*. 2009)

$$F_w(t)=G\sum_{i=1}^{4}\alpha_{wi}\sin(2\pi i f_w t-\theta_{wi}) \tag{4}$$

where G is the walker's weight; α_{wi} is the dynamic amplification factor of the ith harmonic (Table 2); f_w is the walking frequency; and θ_{wi} is the phase lag (Table 2).

Table 2 The values of main dynamic coefficients for the Fourier load function

Harmonic i	α_{wi}	θ_{wi}
1	0.436(f_w-0.95)	0
2	0.006(2f_w+12.3)	π/2
3	0.007(3f_w+5.2)	-π
4	0.007(4f_w+2.0)	-π/2

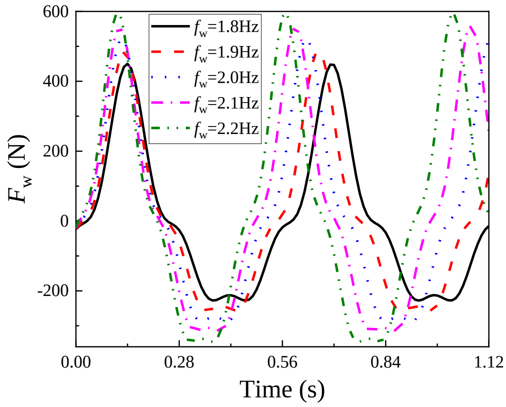

Fig. 1 Fourier load function (G=744.8 N)

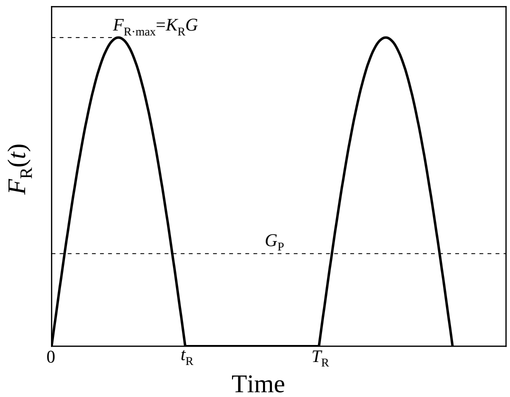

(a) Half-sine model

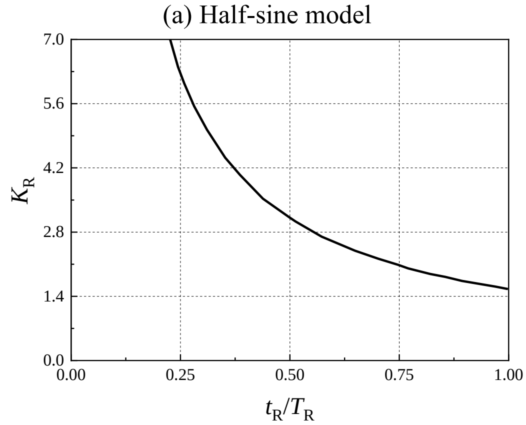

(b) Relationship between K_R and t_R/T_R

Fig. 2 Running force function

In analyzing the acceleration response of the floor system subjected to running excitations, several running forcing functions have also been considered, including the Fourier load function (Chen *et al*. 2012, Occhiuzzi et al. 2008, Schauvliege *et al*. 2014) and half-sine-squared load model (Bachmann and Ammann 1987). For practical reasons, the half-sine-squared load model (Fig. 2) is adopted in this study, which is expressed by

$$F_R(t)=\begin{cases}K_RG\sin(\pi t/t_R) & t\le t_R\\ 0 & t_R\le t\le T_R\end{cases} \tag{5}$$

where K_R (=$F_{p\cdot max}/G$) is the dynamic impact factor; $F_{p\cdot max}$ is the peak dynamic load; t_R is the contact duration; and T_R is the walking duration.

The impact factor K_R results from the condition of constant potential energy, meaning that the integral of the load-time function over one T_R must equalize with the load at rest (static weight). Fig. 2(b) shows how K_R varies with the ratio of t_R/T_R.

3. Acceleration response

Considering the building floor as an anisotropic rectangular plate with length *a* and width *b* (Zhang *et al.* 2017), its vertical response corresponding to a walking or running load (as shown in Fig. 3) can be determined by

$$\begin{aligned} &D_1 \frac{\partial^4 W}{\partial x^4} + 2D_3 \frac{\partial^4 W}{\partial x^2 \partial y^2} + D_2 \frac{\partial^4 W}{\partial y^4} \\ &+ c_d \frac{\partial W}{\partial t} + \frac{q}{g} \frac{\partial^2 W}{\partial t^2} = F(x, y, t) \end{aligned} \tag{6}$$

where c_d is the viscous damping coefficient; D_1 and D_2 are the plate's flexural rigidities in *x* and *y* directions, respectively; D_3 is the combined rigidity; *q* is the floor's weight per unit area; $W = W(x, y, t)$ being the plate's deflection; and $F(x, y, t)$ is the walking or running force function defined by

$$F(x, y, t) = \begin{cases} \sum_{i=1}^{N} \delta(x - x_i, y - y_i) F_w[t - (i-1)t_d] & \text{Walking} \\ \sum_{i=1}^{N} \delta(x - x_i, y - y_i) F_R[t - (i-1)T_R] & \text{Running} \end{cases} \tag{7}$$

where δ is the Dirac Delta function; x_i and y_i are the coordinates of the *i*th step in the *x* and *y* directions, respectively; and t_d is the duration of the contact between foot and floor.

Without the loss of generality, the following sinusoidal function $f(t)$ is adopted to replace walking load function $F_w(t)$ to simplify the calculation:

$$f(t) = f_0 \sin(\omega t) \tag{8}$$

The excitation positions vary during the running time. In analyzing the acceleration response at an arbitrary point (x_R, y_R), the acceleration amplitude is the maximum value when the excitation point is at or near the analysis point. Without the loss of generality, the peak acceleration during the time range $0 \le t \le t_R$ is determined. In this study, the initial condition of the plate is set as

$$W(x, y, 0) = \left. \frac{\partial W(x, y, t)}{\partial t} \right|_{t=0} = 0 \tag{9}$$

To obtain an approximate solution of Eq. (6), the expression of plate's deflection $W(x, y, t)$ can be written as (Mao 2015)

$$W(x, y, t) = \sum_{m=1}^{\infty} \sum_{n=1}^{\infty} T_{mn}(t) W_{mn}(x, y) \tag{10}$$

where $W_{mn}(x, y)$ is the vibration mode function.

Considering the plate's initial condition [i.e. Eq. (9)], the function $T_{mn}(t)$ (m=1, 2, 3, …, n=1, 2, 3, …) must fulfil the following condition:

$$T_{mn}(0) = \left. \frac{dT_{mn}(t)}{dt} \right|_{t=0} = 0 \tag{11}$$

Submitting Eq. (10) into Eq. (6) results in

$$\begin{aligned} &\sum_{m=1}^{\infty} \sum_{n=1}^{\infty} T_{mn} (D_1 \frac{\partial^4 W_{mn}}{\partial x^4} + 2D_3 \frac{\partial^4 W_{mn}}{\partial x^2 \partial y^2} + D_2 \frac{\partial^4 W_{mn}}{\partial y^4}) \\ &+ c_d W_{mn} \frac{dT_{mn}}{dt} + \frac{q W_{mn}}{g} \frac{d^2 T_{mn}}{dt^2} = F(x, y, t) \end{aligned} \tag{12}$$

Eq. (12) must be satisfied for all values of *x* and *y*. However, the solution for each value of *x* and *y* is again impossible to obtain. Thus, it is suggested that $W_{mn}(x, y, t)$ be multiplied and integrate the equation over the plate in *x* and *y* directions. Thus, we obtain

$$\frac{d^2 T_{mn}}{dt^2} + 2\xi_{mn} \omega_{mn} \frac{dT_{mn}}{dt} + \omega_{mn}^2 T_{mn} = Q_{mn} \tag{13}$$

$$\omega_{mn} = \sqrt{\frac{g C_{mn}}{q \Phi_{mn}}}, \quad \xi_{mn} = \frac{g c_d}{2 q \omega_{mn}} \tag{14}$$

$$\Phi_{mn} = \int_0^a \int_0^b W_{mn}^2 dx dy = C_s ab \tag{15}$$

$$\begin{aligned} C_{mn} &= D_1 \int_0^a \int_0^b \frac{\partial^4 W_{mn}}{\partial x^4} W_{mn} dx dy \\ &+ 2D_3 \int_0^a \int_0^b \frac{\partial^4 W_{mn}}{\partial x^2 \partial y^2} W_{mn} dx dy + D_2 \int_0^a \int_0^b \frac{\partial^4 W_{mn}}{\partial y^4} W_{mn} dx dy \end{aligned} \tag{16}$$

$$Q_{mn} = \frac{g}{q \Phi_{mn}} \int_0^a \int_0^b F(x, y, t) W_{mn} dx dy \tag{17}$$

C_s is a coefficient depending on the boundary condition (See Table 4 for details).

Based on the theory of structural dynamics, the solution of (13) is

1) when $\omega_{mn} = \omega$, for walking

$$\begin{aligned} T_{mn}(t) &= \frac{g W_{mn}(x_w, y_w) f_0}{2 \xi_{mn} \omega^2 q \Phi_{mn}} \{ e^{-\xi_{mn} \omega t} [\cos(\omega_{Dmn} t) \\ &+ \frac{\xi_{mn}}{\sqrt{1 - \xi_{mn}^2}} \sin(\omega_{Dmn} t)] - \cos(\omega t) \} \end{aligned} \tag{18}$$

$$\begin{aligned} \frac{d^2 T_{mn}}{dt^2} &= \frac{g W_{mn}(x_w, y_w) f_0}{2 \xi_{mn} q \Phi_{mn}} \{ e^{-\xi_{mn} \omega t} [\frac{\xi_{mn}}{\sqrt{1 - \xi_{mn}^2}} \sin(\omega_{Dmn} t) \\ &- \cos(\omega_{Dmn} t)] + \cos(\omega t) \} \end{aligned} \tag{19}$$

$$\omega_{Dmn} = \omega_{mn} \sqrt{1 - \xi_{mn}^2} \tag{20}$$

For the low damping structure system, the amplitude of sinusoidal item in Eq. (19) can be ignored and $\omega_{Dmn} = \omega$, so Eq. (19) can be simplified as

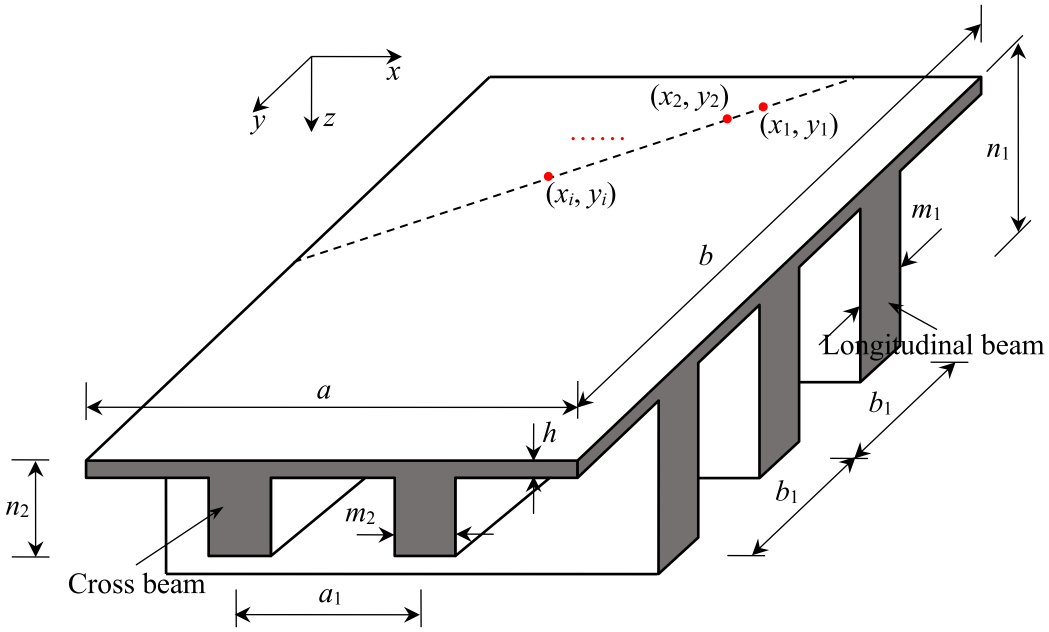

Fig. 3 Anisotropic rectangular floor plate with walking/running points

$$\frac{d^2T_{mn}}{dt^2} \approx \frac{gW_{mn}(x_w, y_w)f_0}{2\xi_{mn}q\Phi_{mn}}(1-e^{-\xi_{mn}\omega t})\cos(\omega t) \tag{21}$$

So the acceleration amplitude $A_{mn\cdot\max}$ is

$$A_{mn\cdot\max} = \frac{\alpha_{wmn} f_0 g}{2C_s\xi qab} \tag{22}$$

$$\alpha_{wmn} = [W_{mn}(x_w, y_w)]^2 \tag{23}$$

where α_{wmn} represents the contribution from the local shape function corresponding to the acceleration amplitude; (x_w, y_w) is the coordinate of arbitrary excitation point; and $W_{mn}(x_w, y_w)$ is the local shape function corresponding to circular frequency ω. If the coefficient α_{wmn} equals to $2C_s e^{-0.35 f_1}$, the Eq. (23) is the computational formula proposed by AISC (Murray et al. 2016).

2) when $\omega_{mn} \neq \omega$, for walking

$$\begin{aligned} T_{mn}(t) = {} & \frac{gW_{mn}(x_w, y_w)f_0}{q\Phi_{mn}[\omega^4 + 2(2\xi_{mn}^2 - 1)\omega^2\omega_{mn}^2 + \omega_{mn}^4]}\{ \\ & \frac{e^{-\xi_{mn}\omega_{mn}t}\omega}{\omega_{Dmn}}\{2\xi_{mn}\omega_{Dmn}\omega_{mn}\cos(\omega_{Dmn}t) + [\omega^2 \\ & +(2\xi_{mn}^2 - 1)\omega_{mn}^2]\sin(\omega_{Dmn}t)\} - 2\xi_{mn}\omega\omega_{mn}\cos(\omega t) \\ & -(\omega^2 - \omega_{mn}^2)\sin(\omega t)\} \end{aligned} \tag{24}$$

$$\begin{aligned} \frac{d^2T_{mn}}{dt^2} = {} & \frac{gW_{mn}(x_w, y_w)f_0}{q\Phi_{mn}[\omega^4 + 2(2\xi_{mn}^2 - 1)\omega^2\omega_{mn}^2 + \omega_{mn}^4]}\{ \\ & \frac{e^{-\xi_{mn}\omega_{mn}t}\omega}{\omega_{Dmn}}\{4\xi_{mn}\omega_{Dmn}\omega_{mn}\cos(\omega_{Dmn}t) + [\omega^2 \\ & +(2\xi_{mn}^2 - 1)\omega_{mn}^2]\sin(\omega_{Dmn}t)\} + 2\xi_{mn}\omega^3\omega_{mn}\cos(\omega t) \\ & -\omega^2(\omega_{mn}^2 - \omega^2)\sin(\omega t)\} \end{aligned} \tag{25}$$

The amplitude of the first term on the righthand side of Eq. (25) depends on initial conditions and the inherent characteristics of the system, which indicates a rapid attenuation of vibration with damping. The second term is caused by steady-state forced vibration. Therefore, Eq. (25) can be simplified as

$$\frac{d^2T_{mn}}{dt^2} = \frac{gW_{mn}(x_w, y_w)f_0[2\xi_{mn}\omega^3\omega_{mn}\cos(\omega t) - \omega^2(\omega_{mn}^2 - \omega^2)\sin(\omega t)]}{q\Phi_{mn}[\omega^4 + 2(2\xi_{mn}^2 - 1)\omega^2\omega_{mn}^2 + \omega_{mn}^4]} \tag{26}$$

and the amplitude is

$$\left(\frac{d^2T_{mn}}{dt^2}\right)_{\max} \approx \frac{gW_{mn}(x_w, y_w)f_0\omega^2}{q\Phi_{mn}\left|\omega^2 - \omega_{mn}^2\right|} \tag{27}$$

So, the acceleration amplitude $A_{mn\cdot\max}$ becomes as

$$A_{mn\cdot\max} = \frac{\alpha_{wmn} f_0 g\omega^2}{C_s qab} \tag{28}$$

$$\alpha_{wmn} = \frac{W_{mn}(x_w, y_w)}{\left|\omega^2 - \omega_{mn}^2\right|} \tag{29}$$

For the walking excitation, the f_0 and ω can be replaced with $\alpha_{wi}G$ and $2\pi i f_w$, respectively.

3) for running

Adopting Duhamel integral results in

$$\begin{aligned} \frac{d^2T_{mn}}{dt^2} = {} & \frac{gW_{mn}(x_R, y_R)}{q\Phi_{mn}\omega_{Dmn}}\frac{e^{-t\xi_{mn}\omega_{mn}}[A_{Rmn}\sin(\omega_{Dmn}t) - B_{Rmn}\cos(\omega_{Dmn}t)]}{\pi^4 + 2\pi^2t_R^2\omega_{mn}^2(2\xi_{mn}^2 - 1) + t_R^4\omega_{mn}^4} \\ & + \frac{gW_{mn}(x_R, y_R)}{q\Phi_{mn}\omega_{Dmn}}\frac{B_{Rmn}\cos(\pi t/t_R) + C_{Rmn}\sin(\pi t/t_R)}{\pi^4 + 2\pi^2t_R^2\omega_{mn}^2(2\xi_{mn}^2 - 1) + t_R^4\omega_{mn}^4} \end{aligned} \tag{30}$$

$$A_{Rmn} = \pi GK_R t_R[\pi^2\omega_{mn}^2(2\xi_{mn}^2 - 1) + t_R^2\omega_{mn}^4] \tag{31}$$

$$B_{Rmn} = 2\pi^3 GK_R t_R\xi_{mn}\omega_{mn}\omega_{Dmn} \tag{32}$$

Table 3 Vibration mode functions for various boundary conditions

Boundary condition	Vibration mode function	k_j: 1	k_j: 2	k_j: $j>2$	Coefficient γ_j
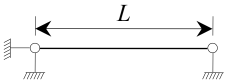	$W_j(z)=\sin k_j z$	$\frac{\pi}{L}$	$\frac{2\pi}{L}$	$\frac{j\pi}{L}$	---
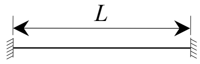	$W_j(z)=\sin k_j z-\sinh k_j z$ $-\gamma_j(\cos k_j z-\cosh k_j z)$	$\frac{4.7300}{L}$	$\frac{7.8532}{L}$	$\frac{(2j+1)\pi}{2L}$	$\frac{\sin k_j L-\sinh k_j L}{\cos k_j L-\cosh k_j L}$
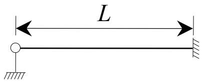	$W_j(z)=\sin k_j z-\gamma_j \sinh k_j z$	$\frac{3.9266}{L}$	$\frac{7.0685}{L}$	$\frac{(4j+1)\pi}{4L}$	$\frac{\sin k_j L}{\sinh k_j L}$
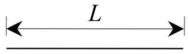	$W_j(z)=\sin k_j z+\sinh k_j z$ $-\gamma_j(\cos k_j z+\cosh k_j z)$	$\frac{4.7300}{L}$	$\frac{7.8532}{L}$	$\frac{(2j+1)\pi}{2L}$	$\frac{\sin k_j L-\sinh k_j L}{\cos k_j L-\cosh k_j L}$

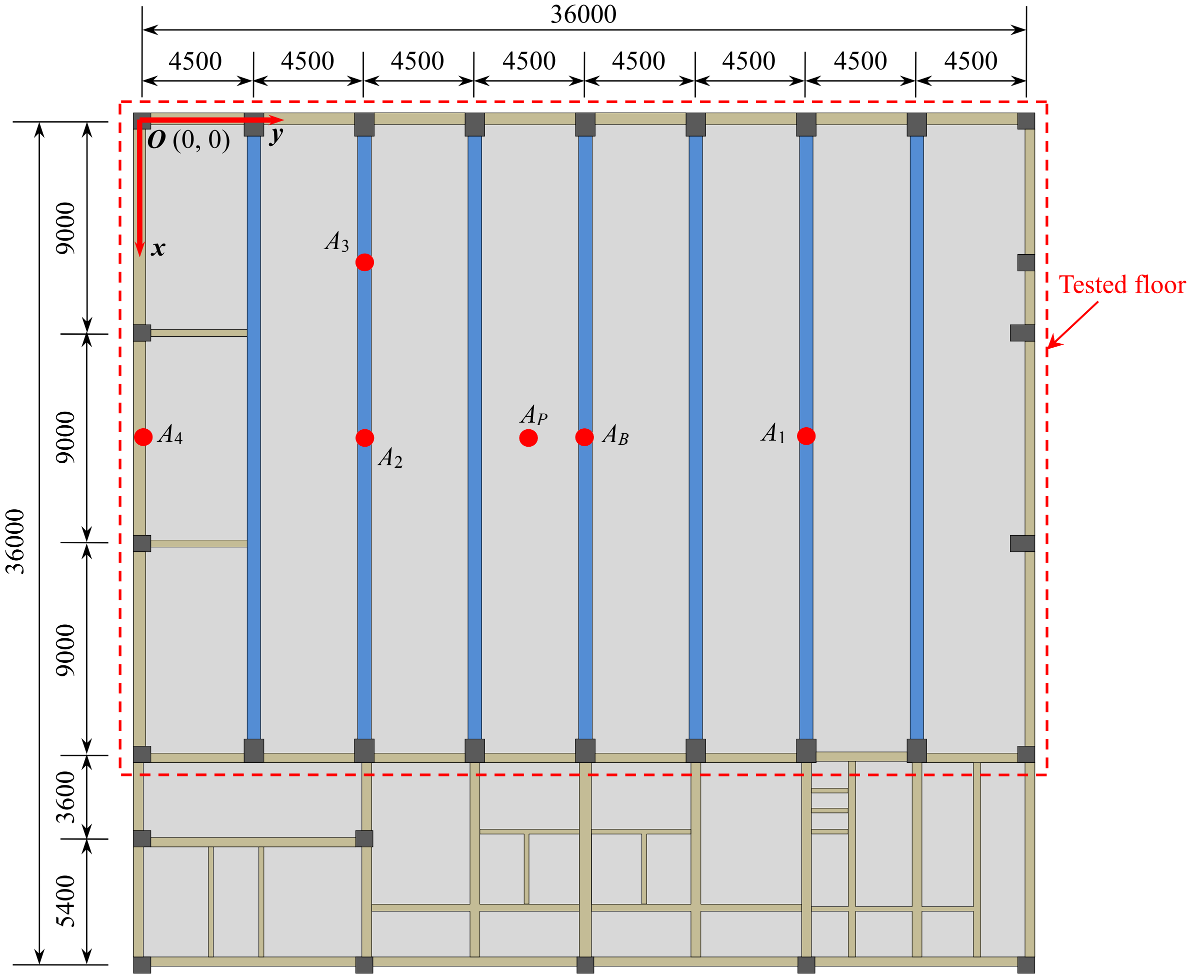

Fig. 4 Outline of prestressed concrete floor #1 (all dimensions in mm)

$$C_{\mathrm{R}mn}=\pi^2 G K_{\mathrm{R}}\omega_{\mathrm{D}mn}(\pi^2-t_{\mathrm{R}}^2\omega_{mn}^2) \tag{33}$$

The vibration induced by the first item on the righthand side of Eq. (30) will decrease quickly with damping; and the vibration induced by the second item is the steady-state forced vibration response. So, Eq. (30) can be simplified as

$$\frac{d^2T_{mn}}{dt^2}=\frac{gW_{mn}(x_{\mathrm{R}},y_{\mathrm{R}})}{q\Phi_{mn}\omega_{\mathrm{D}mn}}\frac{B_{\mathrm{R}mn}\cos(\pi t/t_{\mathrm{R}})+C_{\mathrm{R}mn}\sin(\pi t/t_{\mathrm{R}})}{\pi^4+2\pi^2t_{\mathrm{R}}^2\omega_{mn}^2(2\xi_{mn}^2-1)+t_{\mathrm{R}}^4\omega_{mn}^4} \tag{34}$$

For concrete floors, the damping ratio $\xi_{mn}\approx 2\%$ and $[2(\xi_{mn})^2-1]\approx -1$. Hence, Eq. (34) can be further simplified as

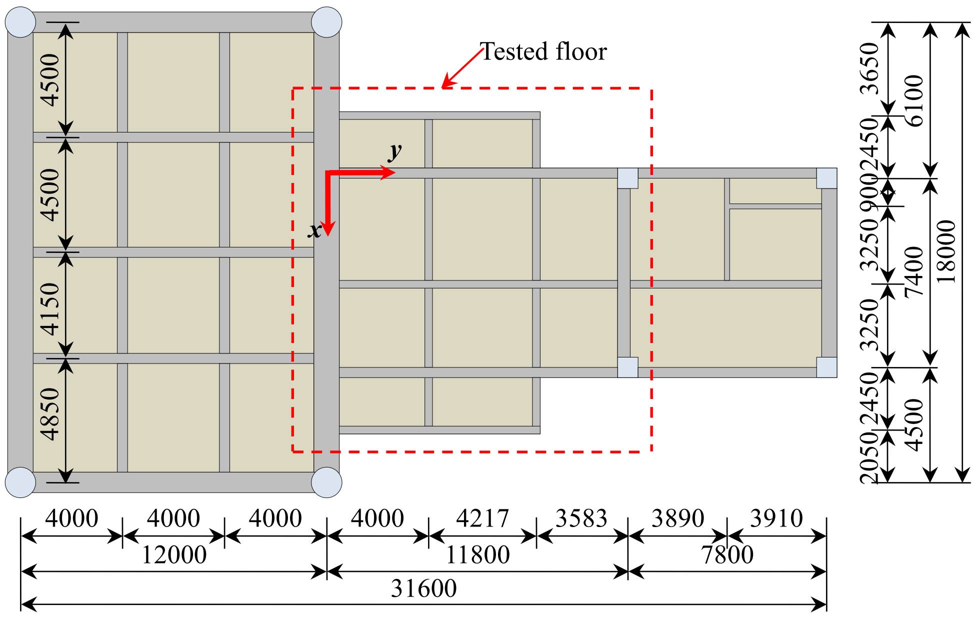

Fig. 5 Outline of prestressed concrete floor #2 (all dimensions in mm)

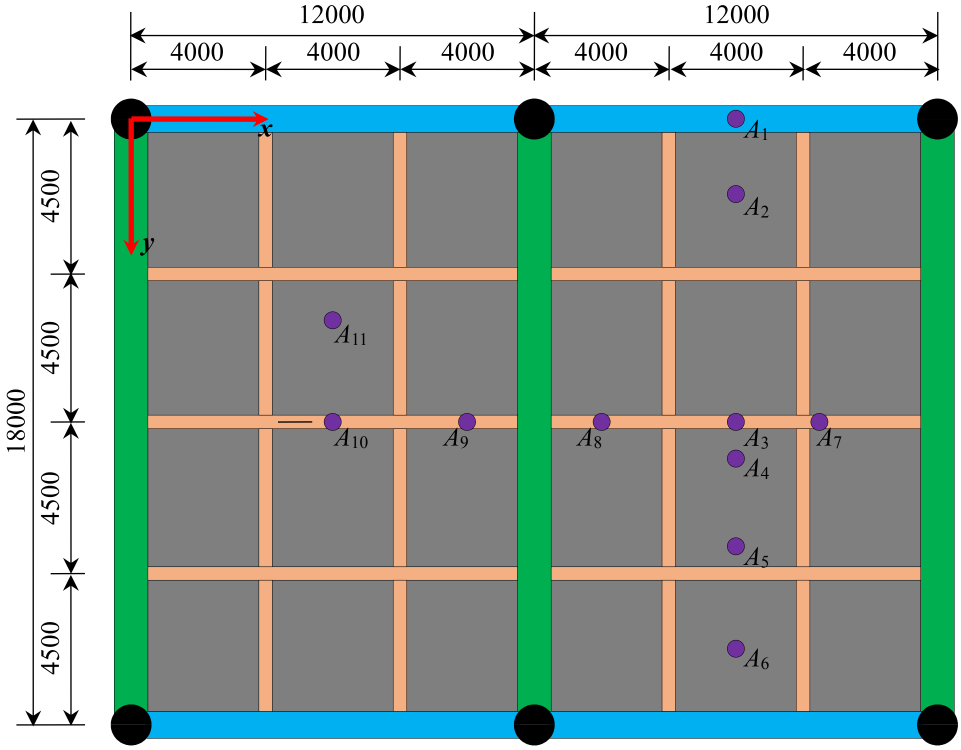

Fig. 6 Outline of prestressed concrete floor #3 (all dimensions in mm)

$$\frac{d^2T_{mn}}{dt^2} = \frac{gW_{mn}(x_R, y_R)GK_R\pi^2}{q\Phi_{mn}(\pi^2 - t_R^2\omega_{mn}^2)^2}[2\pi t_R\xi_{mn}\omega_{mn}\cos(\pi t/t_R) + (\pi^2 - t_R^2\omega_{mn}^2)\sin(\pi t/t_R)] \tag{35}$$

So, the amplitude d^2T_{mn}/dt^2 becomes as

$$\left(\frac{d^2T_{mn}}{dt^2}\right)_{\max} = \frac{gW_{mn}(x_R, y_R)GK_R\pi^2}{q\Phi_{mn}\left|\pi^2 - t_R^2\omega_{mn}^2\right|} \tag{36}$$

And the acceleration amplitude a_p becomes as

$$a_p = \frac{gGK_R\pi^2}{q}\sum_{m=1}^{\infty}\sum_{n=1}^{\infty}\frac{W_{mn}^2(x_R, y_R)}{\Phi_{mn}}\frac{1}{\left|\pi^2 - t_R^2\omega_{mn}^2\right|} = \frac{gGK_R\pi^2}{C_s qab}\sum_{m=1}^{\infty}\sum_{n=1}^{\infty}\frac{W_{mn}^2(x_R, y_R)}{\left|\pi^2 - t_R^2\omega_{mn}^2\right|} \tag{37}$$

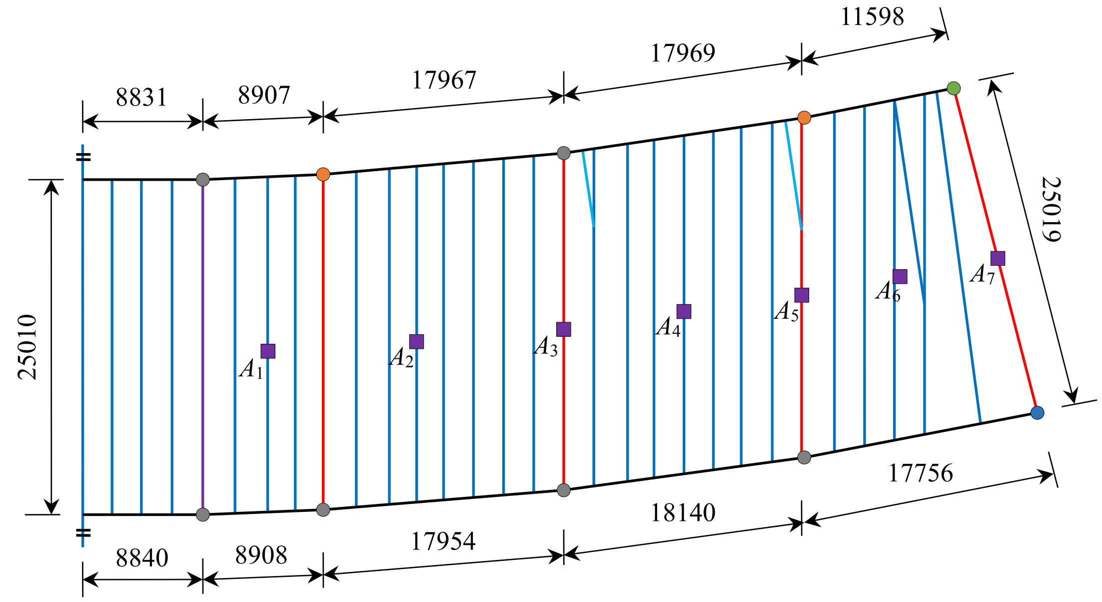

Fig. 7 Outline of prestressed concrete floor #4 (all dimensions in mm)

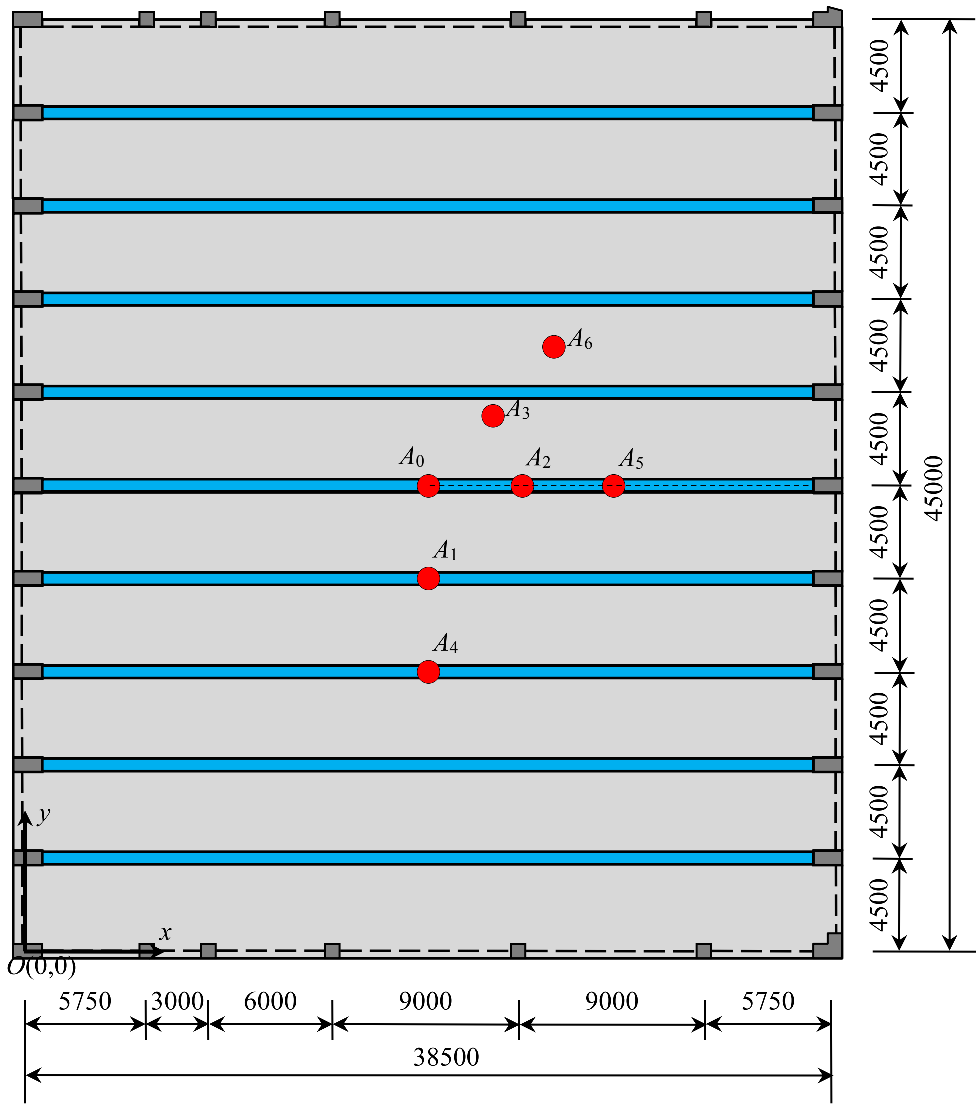

Fig. 8 Outline of prestressed concrete floor #5 (all dimensions in mm)

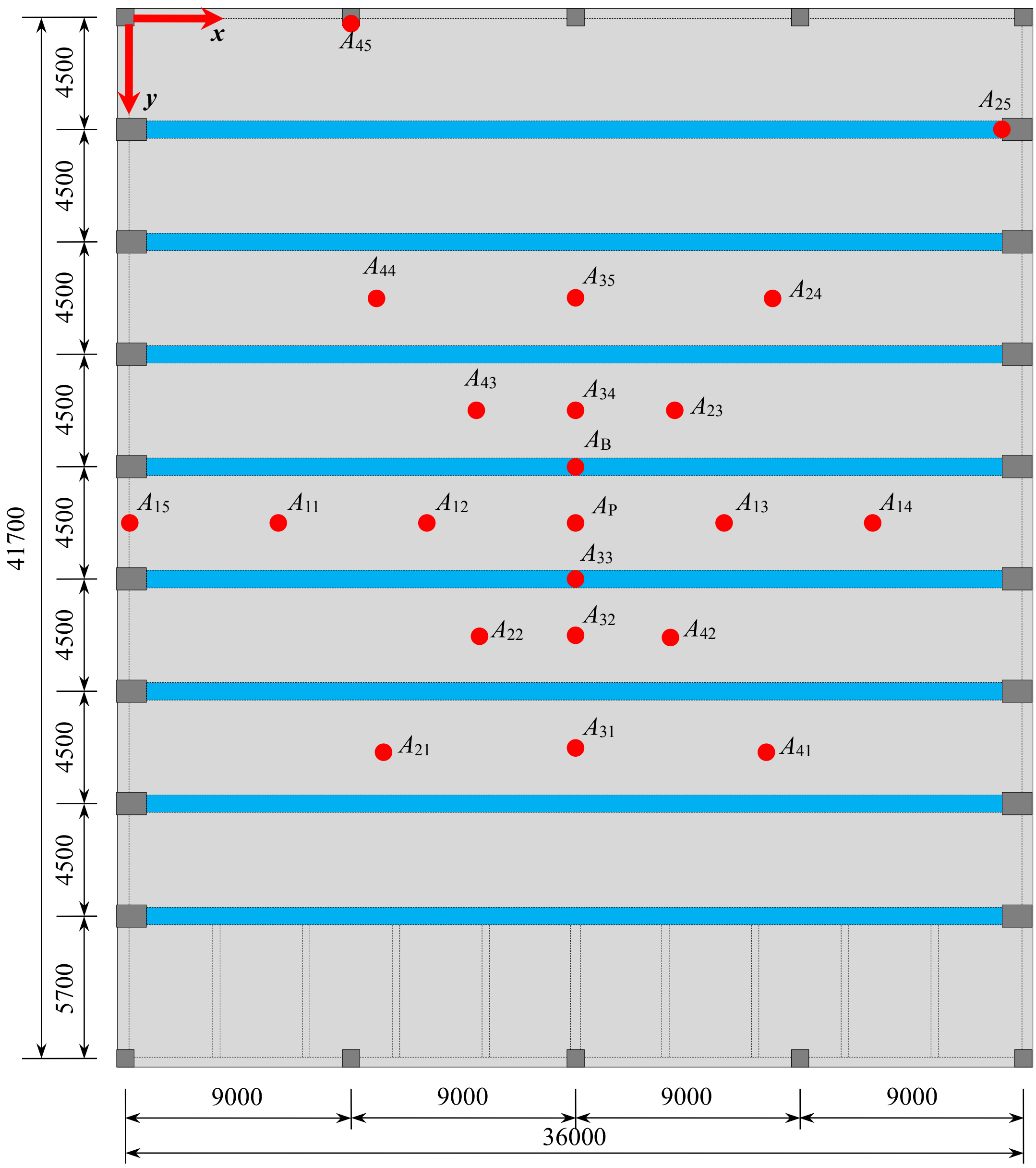

Fig. 9 Outline of prestressed concrete floor #6 (all dimensions in mm)

Let

$$\alpha_{\mathrm{R}} = \frac{1}{C_{\mathrm{s}}} \sum_{m=1}^{\infty} \sum_{n=1}^{\infty} \frac{W_{mn}^{2}(x_{\mathrm{R}}, y_{\mathrm{R}})}{\left|\pi^{2} - t_{\mathrm{R}}^{2} \omega_{mn}^{2}\right|} \tag{38}$$

the Eq. (38) can rewritten as

$$a_{\mathrm{p}} = \frac{\alpha_{\mathrm{R}} g G K_{\mathrm{R}} \pi^{2}}{qab} \tag{39}$$

4. Coefficient determination

For the various boundary conditions of floor system, the function $W_{mn}(x, y)$ (m=1, 2, 3, …, n=1, 2, 3, …) can be written as

$$W_{mn}(x, y) = W_{m}(x) W_{n}(y) \tag{40}$$

where $W_m(x)$ and $W_n(y)$ are respectively the floor's vibration mode shapes in x and y directions, as listed in Table 3.

Table 4 The coefficients of C_{s} of various boundary conditions

Boundary condition	C_{s}
SSSS	1/4
SCSC	1/2
SSSC	1/4
SFSF	1/2
CCCC	1.0
CSCC	1/2
CFCF	1.0
SSCC	1/4
SFCF	1/2

Notes: “S” = simply supported condition; “C” = clamped condition; “F” = free condition.

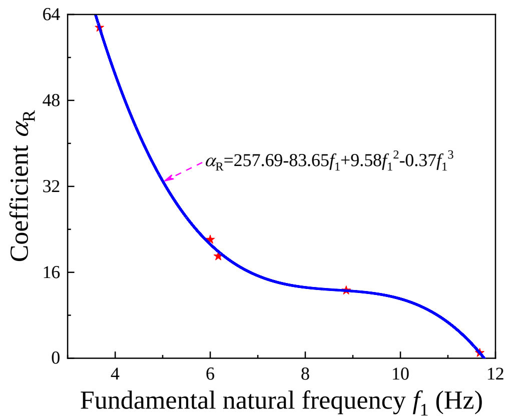

Fig. 10 The relationship between coefficient α_R and fundamental natural frequency f_1 of prestressed concrete floor

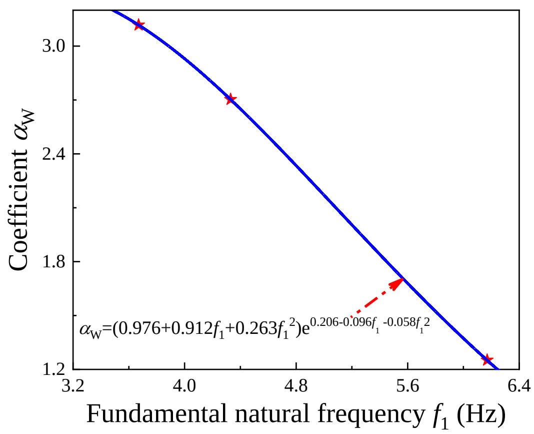

Fig. 11 The relationship between coefficient α_w and fundamental natural frequency f_1 of prestressed concrete floor

Taking Eqs. (15) and (40) into account, coefficient Φ_{mn} for various boundary conditions will be equal to $C_s ab$, where C_s coefficients are listed in Table 4.

It is known that the acceleration amplitude caused by resonant frequency is much higher than other frequencies. So, the peak acceleration amplitude a_p induced by walking [Eqs. (41) and (42)] (Lou *et al.* 2012) or running [Eq. (43)] is

$$a_p = \frac{\alpha_w G g}{\xi q a b} \quad \omega_{mn} = 2\pi i f_w$$
$$\alpha_w = \frac{\alpha_{wmn}\alpha_{wi}}{2C_s} \tag{41}$$

$$a_p = \frac{4\pi^2 f_w^2 \alpha_w g G}{qab} \quad \omega_{mn} \neq \omega_i = 2\pi i f_w$$
$$\alpha_w = [\sum_{i=1}^{4}\sum_{m=1}^{\infty}\sum_{n=1}^{\infty}(\frac{i^2\alpha_{wmn}\alpha_{wi}}{C_s})^{1.5}]^{\frac{1}{1.5}} \tag{42}$$

$$a_p = \frac{\alpha_R g G K_R \pi^2}{qab} \tag{43}$$

A certain number of field tests should be carried out to determine the coefficients α_w (Nonresonant condition) and α_R for obtaining the accurate acceleration amplitude induced by walking or running loads.

In this paper, several prestressed RC floors were investigated experimentally with the outline shown in Fig. 4, Fig. 5, Fig. 6, Fig. 7, Fig. 8 and Fig. 9. Detailed descriptions for prototype floors #1, #2, #3, #4, #5 and #6 are available in the literature Zhou *et al.* (2017b), Cao *et al.* (2018b), Cao *et al.* (2018a), Cao *et al.* (2018c), Zhou *et al.* (2017) and Zhou et al. (2016a).

According to the previous analysis process, the coefficients α_R depend on the mode shape and natural frequencies of the prestressed concrete floor. Based on the experimental results of the prestressed concrete floor 1#, 2#, 3#, 4# and 5#, the calculated coefficients α_R are shown in Fig. 10. It indicates that coefficient α_R vary significantly with fundamental natural frequency f_1 of prestressed concrete floor. For safe and conservative vibration design of a prestressed concrete floor under running loads, the following formulas for α_R coefficient are proposed:

$$\alpha_R = 257.69 - 83.65 f_1 + 9.58 f_1^2 - 0.37 f_1^3 \tag{44}$$

According to the previous analysis process, the coefficients α_w depend on the mode shape, natural frequencies of the prestressed concrete floor and the walking frequency f_w. Based on the experimental results of the prestressed concrete floor 1#, 5# and 6#, the calculated coefficients α_w are shown in Fig. 11. It indicates that coefficient α_w vary significantly with fundamental natural frequency f_1 of prestressed concrete floor. For safe and conservative vibration design of a prestressed concrete floor under walking loads, the following formulas for α_w coefficient are proposed:

$$\alpha_W = (0.976 + 0.912 f_1 + 0.263 f_1^2) e^{(0.206 - 0.096 f_1 - 0.058 f_1^2)} \tag{45}$$

5. Conclusions

The vibration due to walking or running on long-span floor system is studied analytically. For theoretical analysis on the acceleration response [Eqs. (41) and (42) for walking and Eq. (43) for running], the floor system is simplified as an anisotropic rectangular plate and the mode decomposition method is adopted. However, the theoretical formulae are difficult for practical use. For ease and convenience of vibration design, α_w and α_R coefficients equaling to $[\sum_{i=1}^{4}\sum_{m=1}^{\infty}\sum_{n=1}^{\infty}(\frac{i^2\alpha_{wmn}\alpha_{wi}}{C_s})^{1.5}]^{\frac{1}{1.5}}$ and $\sum_{m=1}^{\infty}\sum_{n=1}^{\infty}\frac{W_{mn}^2(x_R, y_R)}{|\pi^2 - t_R^2\omega_{mn}^2|}$ are introduced, which respectively depend on the geometry and support condition of floor system and the contact duration and natural frequency of prestressed concrete floor system. Based on experimental results of six prestressed concrete floor, the coefficients α_w and α_R are proposed

$$\alpha_{\mathrm{W}} = (0.976 + 0.912 f_1 + 0.263 f_1^2) e^{(0.206 - 0.096 f_1 - 0.058 f_1^2)}$$

$$\alpha_{\mathrm{R}} = 257.69 - 83.65 f_1 + 9.58 f_1^2 - 0.37 f_1^3$$

and the acceleration amplitude a_{P} of the floor system under walking or running loads can be more conveniently determined by

$$a_{\mathrm{p}} = \begin{cases} \dfrac{\alpha_{\mathrm{w}} gG}{\xi qab} & \omega_{mn} = 2\pi i f_{\mathrm{w}} \\ \dfrac{4\pi^2 f_{\mathrm{w}}^2 \alpha_{\mathrm{w}} gG}{qab} & \omega_{mn} \neq \omega_i = 2\pi i f_{\mathrm{w}} \end{cases}$$

$$a_{\mathrm{p}} = \frac{\alpha_{\mathrm{R}} gGK_{\mathrm{R}} \pi^2}{qab}$$

Acknowledgments

The authors are grateful for the financial support provided by the National Natural Science Foundation of China (Grant No. 51908084), China Postdoctoral Science Foundation (Grant No. 2020M673139) and Natural Science Foundation of Chongqing, China (Project No. cstc2019jcyj-bshX0013).

References

An, Q., Ren, Q.Y., Liu, H.B., Yan, X.Y. and Chen, Z.H. (2016), "Dynamic performance characteristics of an innovative cable supported beam structure-concrete slab composite floor system under human-induced loads", *Eng. Struct.*, **117**, 40-57. https://doi.org/10.1016/j.engstruct.2016.02.038.

Bachmann, H. and Ammann, W. (1987), *Vibrations in Structures: Induced by Man and Machines*, International Association for Bridge and Structural Engineering, Switzerland.

Bodare, A. and Erlingsson, S. (1993), "Rock music induced damage and vibration at Nya Ullevi Stadium", *Third International Conference on Case Histories in Geotechnical Engineering*, St. Louis, Missouri, June.

Brownjohn, J.M.W., Bocian, M., Hester, D., Quattrone, A., Hudson, W., Moore, D., Goh, S. and Lim, M.S. (2016), "Footbridge system identification using wireless inertial measurement units for force and response measurements", *J. Sound Vib.*, **384**, 339-355. https://doi.org/10.1016/j.jsv.2016.08.008.

Cao, L., Liu, J.P., Li, J. and Zhang, R.Z. (2018a), "Experimental and analytical studies on the vibration serviceability of long-span prestressed concrete floor", *Earthq. Eng. Eng. Vib.*, **17**(2), 417-428. https://doi.org/10.1007/s11803-018-0450-0.

Cao, L., Liu, J.P., Zhou, X.H. and Chen, Y.F. (2018b), "Vibration performance characteristics of a long-span and light-weight concrete floor under human-induced loads", *Struct. Eng. Mech.*, **65**(3), 349-357. https://doi.org/10.12989/sem.2018.65.3.349.

Cao, L., Qi, H.T. and Li, J. (2018c), "Experimental and numerical studies on the vibration serviceability of fanshaped prestressed concrete floor", *Int. J. Distrib. Sens. N.*, **14**(8), 1550147718795746. https://doi.org/10.1177/1550147718795746.

Chen, J., Peng, Y. and Ye, T. (2013), "On methods for extending a single footfall trace into a continuous force curve for floor vibration serviceability analysis", *Struct. Eng. Mech.*, **46**(2), 179-196. https://doi.org/10.12989/sem.2013.46.2.179.

Chen, J., Zhang, M.S. and Liu, W. (2016), "Vibration serviceability performance of an externally prestressed concrete floor during daily use and under controlled human activities", *J. Perform. Constr. Fac.*, **30**, 04015007. https://doi.org/10.1061/(ASCE)CF.1943-5509.0000738.

Chen, X., Ding, Y.L., Li, A.Q., Zhang, Z.Q. and Sun, P. (2012), "Investigations on serviceability control of long-span structures under human-induced excitation", *Earthq. Eng. Eng. Vib.*, **11**(1), 57-71. https://doi.org/10.1007/s11803-012-0098-0.

Da Silva, F.T. and Pimentel, R.L. (2011), "Biodynamic walking model for vibration serviceability of footbridges in vertical direction", *Proceedings of the* 8*th International Conference on Structural Dynamics*, *EURODYN*, Leuven, Belgium, July.

GB 50010-2010 (2010), Code for Design of Concrete Structures; Ministry of Housing and Urban-Rural Development of the People's Republic of China, Beijing, China.

JGJ 3-2010 (2010), Technical Specification for Concrete Structures of Tall Buildings; Ministry of Housing and Urban-Rural Development of the People's Republic of China, Beijing, China.

Liu, J.P., Cao, L. and Chen, Y.F. (2019), "Analytical solution for free vibration of multi-span continuous anisotropic plates by the perturbation method", *Struct. Eng. Mech.*, **69**(3), 283-291. https://doi.org/10.12989/sem.2019.69.3.283.

Liu, J.P., Cao, L. and Chen, Y.F. (2020), "Theoretical analysis of human-structure interaction on seel-concrete composite foors", *J. Eng. Mech.*, **146**(4), 04020007. https://doi.org/10.1061/(ASCE)EM.1943-7889.0001740.

Liu, J.P., Cao, L. and Zhou, Z.K. (2018), "A simplified method for determining acceleration amplitude of prestressed concrete floor under individual jumping load", *Struct. Design Tall Spec. Build.*, **27**(11), e1475. https://doi.org/10.1002/tal.1475.

Lou, Y., Huang, J. and Lv. Z.C. (2012), *Vibration Serviceability Design of Floor System*, Science Press, Beijing.

Lu, X.L., Ding, K., Shi W.X. and Weng, D.G. (2012), "Tuned mass dampers for human-induced vibration control of the Expo Culture Centre at the World Expo 2010 in Shanghai, China", *Struct. Eng. Mech.*, **43**(5), 607-621. https://doi.org/10.12989/sem.2012.43.5.607.

Mao, Q.B. (2015). "AMDM for free vibration analysis of rotating tapered beams", *Struct. Eng. Mech.*, **54**(3), 419-432. https://doi.org/10.12989/sem.2015.54.3.419.

Murray, T.M., Allen, D.E. and Ungar, E.E. (1997), *Steel Design Guide Series No. 11: Floor Vibrations Due to Human Activity*, American Institute of Steel Construction, Inc, Chicago.

Murray, T.M., Allen, D.E., Ungar, E.E. and Davis, D.B. (2016), *Steel Design Guide Series No. 11: Vibrations of Steel-Framed Structural Systems Due to Human Activity* (2nd Edition), American Institute of Steel Construction, Inc, Chicago.

Occhiuzzi, A., Spizzuoco, M. and Ricciardelli, F. (2008), "Loading models and response control of footbridges excited by running pedestrians", *Struct. Control Hlth.*, **15**(3), 349-368. https://doi.org/10.1002/stc.248.

Racic, V. and Brownjohn, J.M.W. (2011), "Stochastic model of near-periodic vertical loads due to humans walking", *Adv. Eng. Inform.*, **25**, 259-275. https://doi.org/10.1016/j.aei.2010.07.004.

Rana, M.M., Brian, U.Y. and Mirza, O. (2015), "Experimental and numerical study of the bond-slip relationship for post-tensioned composite slabs", *J. Constr. Steel Res.*, **114**, 362-379. https://doi.org/10.1016/j.jcsr.2015.08.018.

Schauvliege, C., Verbeke, P., Broeck, P.V.D. and Roeck, G.D. (2014) "Vibration serviceability assessment of a staircase based on moving load simulations and measurements", *Proceedings of the 9th International Conference on Structural Dynamics*, *EURODYN*, Porto, Portugal. July

Shahabpoor, E., Pavic, A. and Racic, V. (2018), "Identification of walking human model using agent-based modelling", *Mech. Syst. Signal Pr.*, **103**, 352-367. https://doi.org/10.1016/j.ymssp.2017.10.028.

Shahabpoor, E., Pavic, A., Racic, V. and Zivanovic, S. (2017), "Effect of group walking traffic on dynamic properties of pedestrian structures", *J. Sound Vib.*, **387**, 207-225. https://doi.org/10.1016/j.jsv.2016.10.017.

Smith, A.L., Hicks, S.J. and Devine, P. J. (2009), *Design of Floors for Vibration*: *A New Approach*, The Steel Construction Institute, Berkshire, United Kingdom.

Wang, J.P. and Chen, J. (2017), "A comparative study on different walking load models", *Struct. Eng. Mech.*, **63**(6), 847-856. https://doi.org/10.12989/sem.2017.63.6.847.

Wilden, H. (Ed.) (2010), *PCI Design Handbook*: *Precast and Prestressed Concrete* (7th edition), Precast/Prestressed Concrete Institute, Chicago, USA.

Zhang, S.G., Xu, L. and Qin, J.W. (2017), "Vibration of lightweight steel floor systems with occupants: Modelling, formulation and dynamic properties", *Eng. Struct.*, **147**, 652-665. https://doi.org/10.1016/j.engstruct.2017.06.008.

Zhou, X.H., Cao, L., Chen, Y.F., Liu, J.P. and Li, J. (2016a), "Acceleration response of prestressed cable RC truss floor system subjected to heel-drop loading", *J. Perform. Constr. Facil.*, **30**(5), 04016014. https://doi.org/10.1061/(ASCE)CF.1943-5509.0000864.

Zhou, X.H., Cao, L., Chen, Y.F., Liu, J.P. and Li, J. (2016b), "Experimental and analytical studies on the vibration serviceability of pre-stressed cable RC truss floor systems", *J. Sound Vib.*, **361**, 130-147. http://dx.doi.org/10.1016/j.jsv.2015.10.001.

Zhou, X.H., Li, J., Liu, J.P. and Chen, Y.F. (2017a), "Dynamic performance characteristics of pre-stressed cable RC truss floor system under human-induced loads", *Int. J. Struct. Stab. Dy.*, **17**(4), https://doi.org/1750049. 10.1142/S0219455417500493.

Zhou, X.H., Liu, J.P., Cao, L. and Li, J. (2017b), "Vibration serviceability of pre-stressed concrete floor system under human activity", *Struct. Infrastruct. E.*, **13**(8), 967-977. https://doi.org/10.1080/15732479.2016.1229796.

Zivanovic, S., Pavic A. and Reynolds, P. (2005). "Vibration serviceability of footbridges under human-induced excitation: a literature review", *J. Sound Vib.*, **279**, 1-74. https://doi.org/10.1016/j.jsv.2004.01.019.

CC